ANTICANCER RESEARCH *38*: 3897-3906 (2018)
doi:10.21873/anticanres.12674

Quantitative Structure–Cytotoxicity Relationship of 2-(*N*-cyclicamino)chromone Derivatives

HAIXIA SHI[1,2], JUNKO NAGAI[3], TSUKASA SAKATSUME[4], KENJIRO BANDOW[5], NORIYUKI OKUDAIRA[6], HIROSHI SAKAGAMI[2], MINEKO TOMOMURA[5], AKITO TOMOMURA[5], YOSHIHIRO UESAWA[3], KOICHI TAKAO[4] and YOSHIAKI SUGITA[4]

[1]Department of Traditional Chinese Medicine, Shanghai Ninth People's Hospital, Shanghai Jiatong University School of Medicine, Shanghai, P.R. China;
[2]Meikai University Research Institute of Odontology (M-RIO), Saitama, Japan;
[3]Department of Medical Molecular Informatics, Meiji Pharmaceutical University, Tokyo, Japan;
[4]Department of Pharmaceutical Sciences, Faculty of Pharmacy and Pharmaceutical Sciences, Josai University, Saitama, Japan;
Divisions of [5]Biochemistry and [6]Pharmacology, Meikai University School of Dentistry, Saitama, Japan

Abstract. *Background/Aim: 4H-1-Benzopyran-4-ones (chromones) have provided backbone structure for the chemical synthesis of potent anticancer drugs. In this study, the cytotoxicity of fifteen 2-(N-cyclicamino)chromone derivatives was investigated and subjected to quantitative structure–activity relationship (QSAR) analysis. Materials and Methods: Cytotoxicity against four human oral squamous cell carcinoma cell lines and three oral normal mesenchymal cells was determined by the 3-(4,5-dimethylthiazol-2-yl)-2,5-diphenyltetrazolium bromide (MTT) method. Tumor specificity (TS) was evaluated by ratio of mean 50% cytotoxic concentration (CC_{50}) against normal oral cells to that against human oral squamous cell carcinoma cell lines. Potency-selectivity expression (PSE) value was calculated by dividing the TS value by CC_{50} against tumor cells. Apoptosis induction was evaluated by morphological observation, western blot analysis and cell- cycle analysis. For QSAR analysis, a total of 3,089 physicochemicals, structural and quantum chemical features were calculated from the most stabilized structure optimized using Corina. Results: 7-Methoxy-2-(4-morpholinyl)-4H-1-benzopyran-4-one (**5c**) showed highest tumor-specificity, comparable with that of doxorubicin, without inducing apoptosis. Tumor-specificity of fifteen 2-(N-cyclicamino) chromones was correlated with molecular shape, especially 3D-structure. Conclusion: Chemical modification of **5c** may be a potential choice for designing a new type of anticancer drugs.*

Correspondence to: Haixia Shi, Department of Traditional Chinese Medicine, Shanghai Ninth People's Hospital, Shanghai Jiatong University School of Medicine, 280, Mohe Road, Shanghai, 201900, P.R. China. Tel: +86 21 56691101 ext 6627, e-mail: haixia.0101@163.com; Hiroshi Sakagami, Meikai University Research Institute of Odontology (M-RIO), 1-1 Keyakidai, Sakado, Saitama 350-0283, Japan. Tel: +81 492792758 (office), +81 492792787 (M-RIO) (dial-in), Fax: +81 492855171, e-mail: sakagami@dent.meikai.ac.jp

Key Words: 2-(*N*-Cyclicamino)chromones, QSAR analysis, cytotoxicity, tumor selectivity, molecular shape.

4*H*-1-Benzopyran-4-one (chromone) are an important class of oxygenated heterocyclic compounds, since the core structure is found ubiquitously in the plant kingdom in notable amounts (1), and thus provides a backbone structure for the synthesis of various derivatives. 2-Aminochromone derivatives showed various biological activities including anti-inflammatory activity (2, 3), antimicrobial activity (3), phosphodiesterase inhibition (4, 5), modulation of DNA repair (6), inhibitors of DNA-dependent protein kinase and radiosensitization of a human tumor cell line (7) and new potential PET agents for imaging of DNA-dependent protein kinase (DNA-PK) in cancer (8). On the other hand, the investigation of their anticancer activity, using both human malignant and non-malignant cells, is limited.

We recently reported that (*E*)-3-[2-(4-hydroxyphenyl) ethenyl]-6-methoxy-4*H*-1-benzopyran-4-one (classified as 3-styrylchromones) (9), (*E*)-3-[2-(4-chlorophenyl)ethenyl]-7-methoxy-2*H*-1-benzopyran (classified as 3-styryl-2*H*-chromenes) (10), 2-(1*H*-indol-1-yl)-4*H*-1-benzopyran-4-one, 2-(1*H*-indol-1-yl)-7-methoxy-4*H*-1-benzopyran-4-one and 2-(1*H*-indol-1-yl)-6-methoxy-4*H*-1-benzopyran-4-one (classified as 2-azolylchromones) (11), showed much higher cytotoxicity against human oral squamous cell carcinoma (OSCC) cell lines than against human normal oral mesenchymal normal oral cells (gingival fibroblast, periodontal ligament fibroblast, pulp cell),

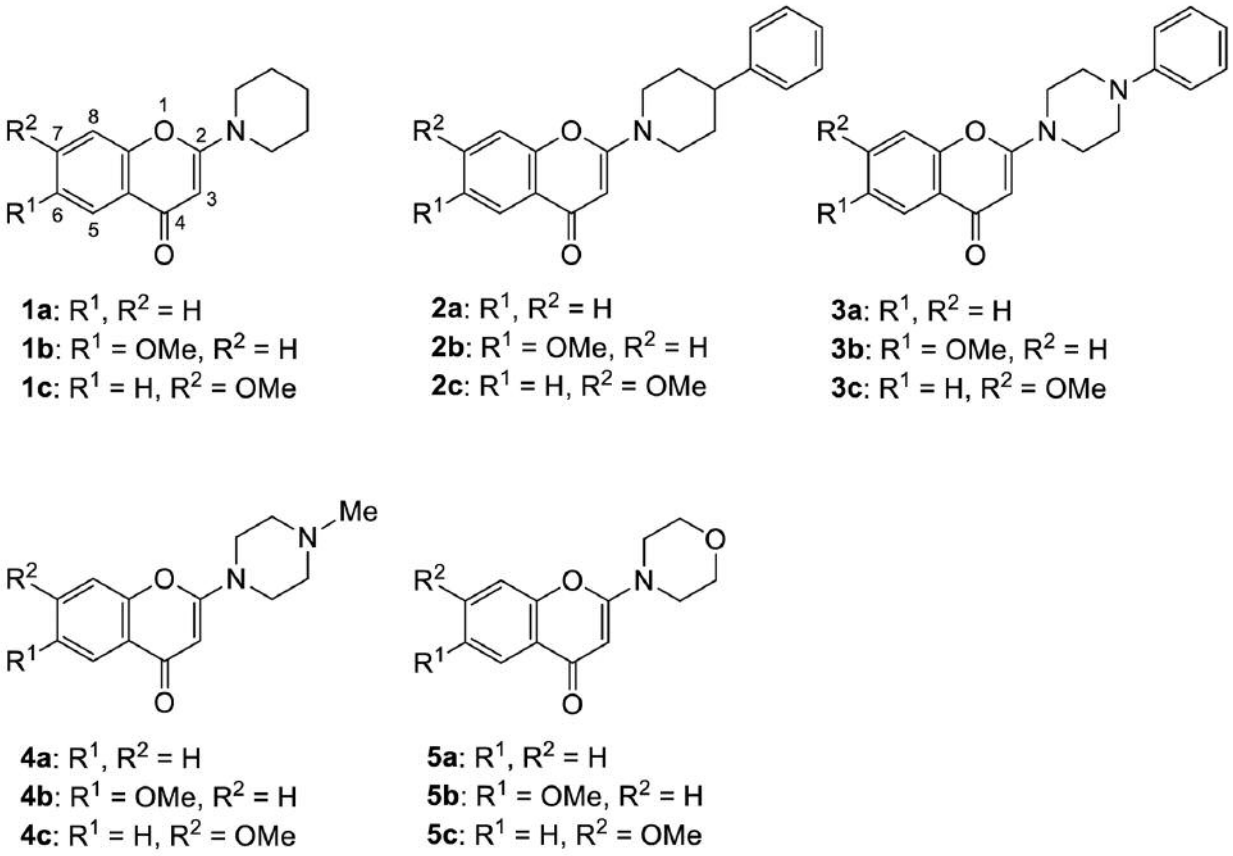

Figure 1. *Structure of fifteen 2-(N-cyclicamino)chromones.*

yielding excellent tumor-specificity (TS) (TS=69, 60, >38, 24 and 24, respectively) (9-11) comparable with that of anti-cancer drugs (camptothecin, S*N*-38, doxorubicin, daunorubicin, etoposide, mitomycin C, 5-fluorouracil, docetaxel, melphalan and gefitinib) (TS=>1853, >979, 70, 55, 93, 31, >170, >10, >2708 and 4, respectively) (12). Furthermore, (*E*)-3-[2-(4-hydroxyphenyl)ethenyl]-6-methoxy-4*H*-1-benzopyran-4-one (9), and (*E*)-3-[2-(4-chlorophenyl)ethenyl]-7-methoxy-2*H*-1-benzopyran (10) showed much lower cytotoxicity against human normal oral epithelial cells (9, 10) as compared with these anticancer drugs (12).

In continuation of discovering new biological activities of chromone derivatives, a total of fifteen 2-(*N*-cyclicamino) chromone derivatives (Figure 1) were investigated for their cytotoxicity against four human OSCC cell lines and three human normal oral cells, and then subjected to quantitative structure–activity relationship (QSAR) analysis.

Materials and Methods

Materials. The following chemicals and reagents were obtained from the indicated companies: Dulbecco's modified Eagle's medium (DMEM), from GIBCO BRL (Grand Island, NY, USA); fetal bovine serum (FBS), 3-(4,5-dimethylthiazol-2-yl)-2,5-diphenyltetrazolium bromide (MTT), doxorubicin, ribonuclease (RNase) A from Sigma-Aldrich Inc. (St. Louis, MO, USA); propidium iodide (PI), dimethyl sulfoxide (DMSO), actinomycin D (Act. D), 4% paraformaldehyde phosphate buffer solution (Wako Pure Chem. Ind., Osaka, Japan); Nonidet P-40 (NP-40) (Nakalai Tesque Inc., Kyoto, Japan); Culture plastic dishes and 96-well plates (TPP, Techno Plastic Products AG, Trasadingen, Switzerland).

Synthesis of 2-(N-cyclicamino)chromone derivatives. 2-(1-Piperidinyl)-4*H*-1-benzopyran-4-one (**1a**), 6-methoxy-2-(1-piperidinyl)-4*H*-1-benzopyran-4-one (**1b**), 7-methoxy-2-(1-piperidinyl)-4*H*-1-benzopyran-4-one (**1c**), 2-(4-phenyl-1-piperidinyl)-4*H*-1-benzopyran-4-one (**2a**), 6-methoxy-2-(4-phenyl-1-piperidinyl)-4*H*-1-benzopyran-4-one (**2b**), 7-methoxy-2-(4-phenyl-1-piperidinyl)-4*H*-1-benzopyran-4-one (**2c**), 2-(4-phenyl-1-piperazinyl)-4*H*-1-benzopyran-4-one (**3a**), 6-methoxy-2-(4-phenyl-1-piperazinyl)-4*H*-1-benzopyran-4-one (**3b**), 7-methoxy-2-(4-phenyl-1-piperazinyl)-4*H*-1-benzopyran-4-one (**3c**), 2-(4-methyl-1-piperazinyl)-4*H*-1-benzopyran-4-one (**4a**), 6-methoxy-2-(4-methyl-1-piperazinyl)-4*H*-1-benzopyran-4-one (**4b**), 7-methoxy-2-(4-methyl-1-piperazinyl)-4*H*-1-benzopyran-4-one (**4c**), 2-(4-morpholinyl)-4*H*-1-benzopyran-4-one (**5a**), 6-methoxy-2-(4-morpholinyl)-4*H*-1-benzopyran-4-one (**5b**), 7-methoxy-2-(4-morpholinyl)-4*H*-1-benzopyran-4-one (**5c**) were synthesized by the nucleophilic substitution reactions of 3-triazolylchromone derivatives

Table I. *Cytotoxic activity of fifteen 2-(N-cyclicamino)chromones against oral malignant and non-malignant cells. Each value represents the mean of triplicate determinations. Two sets of TS and PSE values were determined using all malignant and non-malignant cells, or the pair of the cells derived from the same (gingival) tissue.*

	CC_{50} (μM)											TS		PSE	
	Human oral squamous cell carcinoma cell lines						Human normal oral cells								
	Ca9-22 A	HSC-2	HSC-3	HSC-4	mean B	SD	HGF C	HPLF	HPC	mean D	SD	D/B	C/A	$(D/B_2)\times100$	$C/A_2)\times100$
1a	391	400	400	400	398	5	299	400	400	366	59	0.9	0.8	0.23	0.20
1b	400	400	325	382	377	35	341	350	400	364	32	1.0	0.9	0.26	0.21
1c	400	396	400	366	391	16	275	361	400	345	64	0.9	0.7	0.23	0.17
2a	248	279	348	255	282	46	268	220	195	228	37	0.8	1.1	0.29	0.44
2b	400	400	400	400	400	0	400	400	400	400	0	1.0	1.0	0.25	0.25
2c	400	400	359	400	390	21	292	271	367	310	51	0.8	0.7	0.20	0.18
3a	121	126	174	97	130	32	242	260	173	225	46	1.7	2.0	1.34	1.64
3b	286	280	199	209	243	46	263	266	274	268	6	1.1	0.9	0.45	0.32
3c	85	76	119	91	93	19	196	229	400	275	110	3.0	2.3	3.18	2.69
4a	400	400	400	400	400	0	400	400	388	396	7	1.0	1.0	0.25	0.25
4b	400	400	400	400	400	0	400	400	400	400	0	1.0	1.0	0.25	0.25
4c	400	400	400	393	398	4	400	400	400	400	0	1.0	1.0	0.25	0.25
5a	345	312	400	360	354	36	400	400	154	318	142	0.9	1.2	0.25	0.34
5b	400	258	400	326	346	68	392	400	400	397	5	1.1	1.0	0.33	0.25
5c	**9.1**	**6.0**	**3.7**	**3.1**	**5.5**	**2.7**	**244**	**400**	**400**	**348**	**90**	**63.4**	**26.7**	**1156.34**	**291.68**
DXR	0.21	0.06	0.15	0.19	0.15	0.06	6.84	6.87	7.95	7.22	0.63	48.3	33.2	32349.05	16165.43

HGF: Human gingival fibroblast; HPLF: human periodontal ligament fibroblast; HPC: human pulp cells; Ca9-22 (derived from gingival tissue), HSC-2, HSC-3 and HSC-4 (derived from tongue), oral squamous cell carcinoma cell lines; CC_{50}: 50% cytotoxic concentration; DXR: doxorubicin; TS: tumor-selectivity index; PSE: potency-selectivity expression.

(13) with selected cyclic secondary amines, according to previous methods (14). All compounds were dissolved in DMSO at 40 mM and stored at –20˚C before use.

Cell culture. Human normal oral mesenchymal cells (human gingival fibroblast, HGF; human periodontal ligament fibroblast, HPLF; human pulp cells, HPC) were established from the first premolar tooth extracted from the lower jaw of a 12-year-old girl (15), and cells at 10-18 population doubling levels were used in this study. Human oral squamous cell carcinoma (OSCC) cell lines [Ca9-22 (derived from gingival tissue); HSC-2, HSC-3, HSC-4 (derived from tongue)] were purchased from Riken Cell Bank (Tsukuba, Japan). All of these cells were cultured at 37˚C in DMEM supplemented with 10% heat-inactivated FBS, 100 units/ml, penicillin G and 100 μg/ml streptomycin sulfate under a humidified 5% CO_2 atmosphere. Cell morphology was checked periodically under the light microscope (EVOS FL, ThermoFisher Scientific, Waltham, MA, USA).

Assay for cytotoxic activity. Cells were inoculated at 2×10^3 cells/0.1 ml in a 96-microwell plate. After 48 h, the medium was replaced with 0.1 ml of fresh medium containing different concentrations of single test compounds. Cells were incubated further for 48 h and the relative viable cell number was then determined by the MTT method (9-12). The relative viable cell number was determined by the absorbance of the cell lysate at 560 nm, using a microplate reader (Infinite F50R, TECAN, Männedorf, Switzerland). Control cells were treated with the same amounts of DMSO and the cell damage induced by DMSO was subtracted from that induced by test agents. The concentration of compound that reduced the viable cell number by 50% (CC_{50}) was determined from the dose–response curve and the mean value of CC_{50} for each cell type was calculated from triplicate assays.

Calculation of tumor-selectivity index (TS). TS was calculated using the following equation: TS=mean CC_{50} against three normal oral cells/mean CC_{50} against for OSCC cell lines [(D/B) in Table I]. Since both Ca9-22 and HGF cells were derived from the gingival tissue (16), the relative sensitivity of these cells was also compared [(C/A) in Table I].

Calculation of potency-selectivity expression (PSE). PSE was calculated by the following equation: PSE=TS/CC_{50} against tumor cells ×100 [that is, (D/B^2) ×100 (HGF, HPLF, HPC *vs*. Ca9-22, HSC-2, HSC-3, HSC-4) using all non-malignant and malignant cells, and (C/A^2) ×100 (HGF *vs*. Ca9-22) using the pair of the cells from the same tissue (gingiva) (Table I).

Western blot analysis. Cells were washed with phosphate-buffered saline (PBS) and re-suspended in 50 mM Tris-HCl (pH 7.6), 150 mM NaCl, 1 mM EDTA, 0.1% sodium dodecyl sulfate (SDS), 0.5% deoxycholic acid, 1% NP-40 and protease inhibitors (RIPA buffer). After ultrasonication using Bioruptor (UCD-250; Cosmo Bio, Tokyo, Japan) for 12.5 min (10 sec on, 20 sec off) at the middle level of output (250 W) at 4˚C, the soluble cellular extracts were

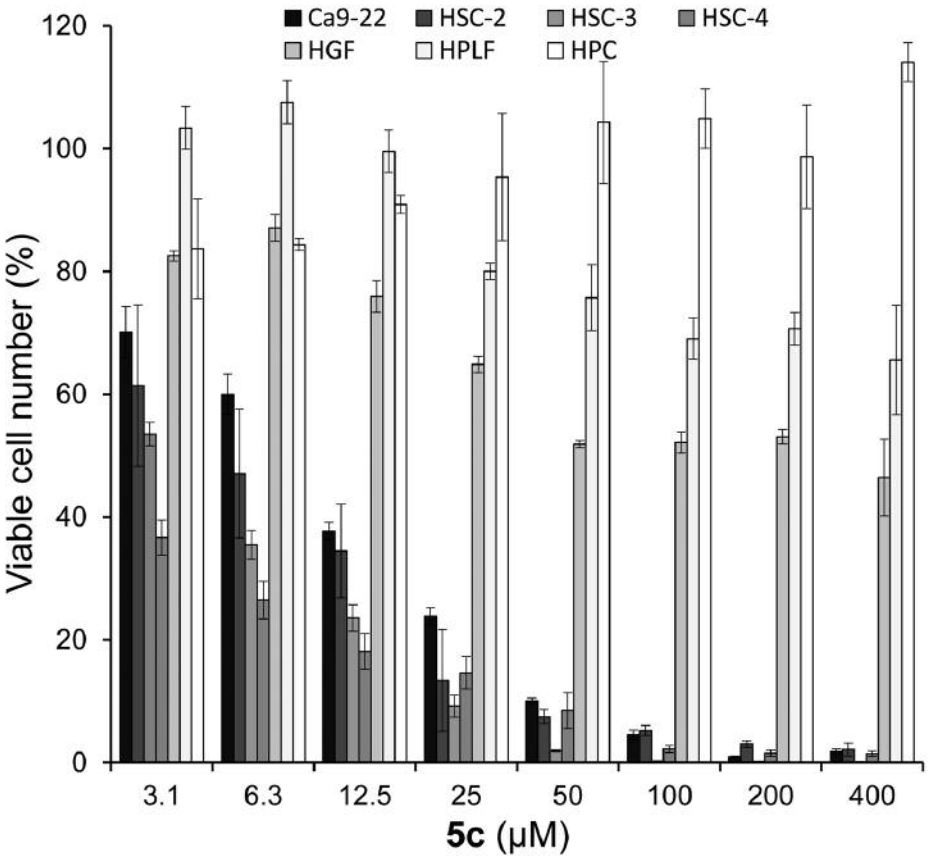

Figure 2. *Cytotoxicity of* ***5c*** *against four human OSCC cells lines and human normal oral cells. Ca9-22, HSC-2, HSC-3, HSC-4, HGF, HPLF and HPC (indicated by decreasing intensity of black color) were incubated for 48 h without (control) or with the indicated concentrations of* ***5c****, and cell viability was determined by MTT method, and expressed as % of control. Each value represents mean±S.D. of triplicate assays.*

recovered after centrifugation for 10 min at 16,000 × *g*. The protein concentration of each sample was determined using the BCA Protein Assay Reagent Kit (Thermo Fisher Scientific) and cell extracts were subjected to Western blot (WB) analysis. The blots were probed with anti- Poly (ADP-ribose) polymerase (PARP) antibody (Cell Signaling Technology Inc., Beverly, MD, USA), anti-caspase 3 antibody (Cell Signaling Technology Inc.), or anti-glyceraldehyde 3-phosphate dehydrogenase (GAPDH) antibody (Trevigen, Gaithersburg, MD, USA), followed by a horseradish peroxidase-conjugated anti-α-rabbit IgG secondary antibody (DAKO, Glostrup, Denmark). The immune complexes were visualized using Pierce Western Blotting Substrate Plus (Thermo Fisher Scientific). WB results were documented and quantified using ImageQuant LAS 500 (GE Healthcare, Tokyo, Japan) (17).

Cell cycle analysis. Cells (approximately 10^6 cells) were harvested, fixed with 1% paraformaldehyde in phosphate-buffered saline without calcium and magnesium ions [PBS (–)]. Fixed cells were washed twice with PBS (–), and then treated for 30 min with 200 μl of 2 mg/ml RNase A (preheated for 10 min at 100˚C to inactivate DNase) to degrade RNA. Cells were then washed twice with PBS (–) and stained for 15 min with 0.01% propidium iodide (PI) in the presence of 0.01% NP-40 in PBS (–) that prevents cell aggregation. After filtering through Falcon® cell strainers (40 μM) (Corning, NY, USA) to remove aggregated cells, PI-stained cells were subjected to cell sorting (SH800 Series, SONY Imaging Products and Solutions Inc., Atsugi, Kanagawa, Japan). Cell cycle analysis was performed with Cell Sorter Software version 2.1.2. SONY Imaging Products and Solution Inc.).

Estimation of CC_{50} values. Since the CC_{50} values had a distribution pattern close to a logarithmic normal distribution, we used the pCC_{50} (*i.e.*, the $-\log CC_{50}$) for the comparison of the cytotoxicity between the compounds. The mean pCC_{50} values for normal cells and tumor cell lines were defined as N and T, respectively (10).

Calculation of chemical descriptors. The 3D-structure of each chemical structure (drawn by Marvin Sketch ver 16, ChemAxon, Budapest, Hungary, http://www.chemaxon.com) was optimized by CORINA Classic (Molecular Networks GmbH, Nürnberg, Germany) with forcefield calculations (amber-10: EHT) in Molecular Operating Environment (MOE) version 2018.0101 (Chemical Computing Group Inc., Quebec, Canada). The number of structural descriptors calculated from MOE (18) and Dragon 7.0 (19) (Kode srl., Pisa, Italy) after the elimination of overlapped descriptors were 293 and 2,796, respectively.

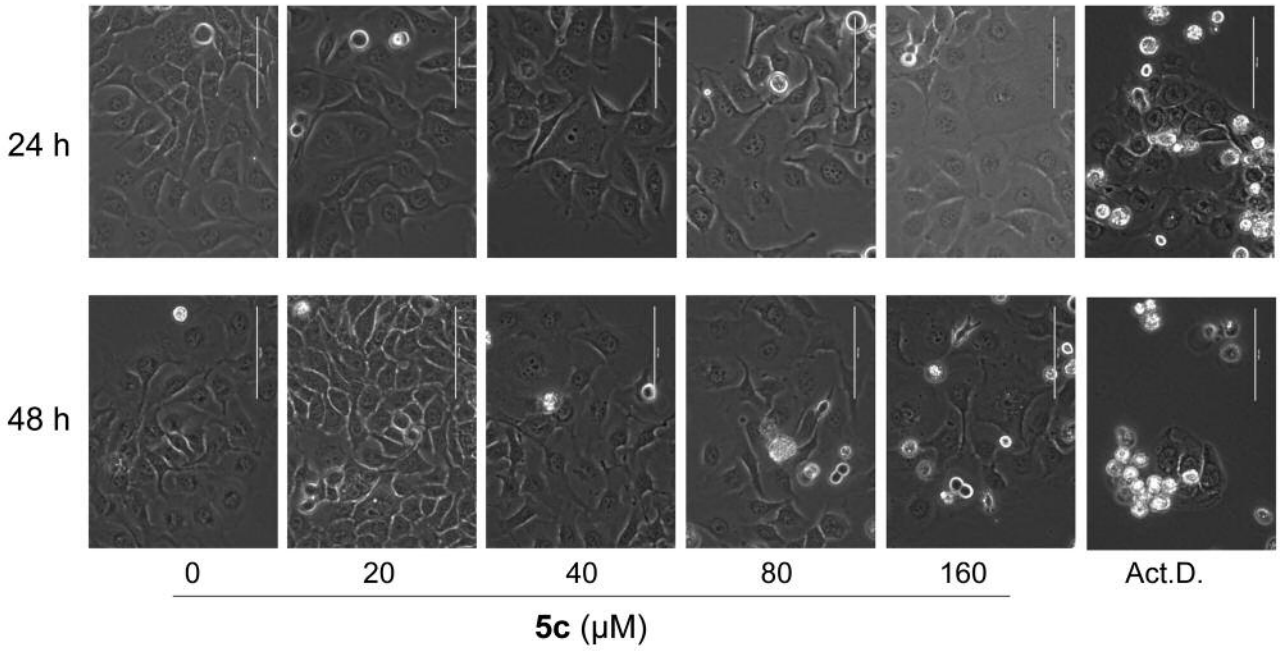

Figure 3. *Production of enlarged cell population by* ***5c*** *in HSC-2 cells. HSC-2 cells were incubated for 24 or 48 h with the indicated concentrations of* ***5c*** *or 1 μM actinomycin D (Act. D, positive control), and then assessed for morphology under the light microscope (EVOS FL, ThermoFisher Scientific). Bar: 100 μm.*

Statistical treatment. The relation among cytotoxicity, tumor specificity index and chemical descriptors was investigated using simple regression analyses by JMP Pro version 13.2.0 (SAS Institute Inc., Cary, NC, USA). The significance level was set at $p<0.05$.

Results

Cytotoxicity. A total of fifteen 2-(*N*-cyclicamino)chromone derivatives were synthesized, without (a series) or with introduction of methoxy group at the C-6 position (b series) or the C-7 position (c series) of benzopyran-4-one (chromone) ring attached by 1-piperidinyl (**1a**, **1b**, **1c**), 4-phenyl-1-piperidinyl (**2a**, **2b**, **2c**), 4-phenyl-1-piperazinyl (**3a**, **3b**, **3c**), 4-methyl-1-piperazinyl (**4a**, **4b**, **4c**) or 4-morpholinyl (**5a**, **5b**, **5c**) group at the C-2 position (Figure 1).

The effect of introduction of substituent groups at the C-2 position was first investigated on the cytotoxicity induction of chromone. Compound introduced with 4-phenyl-1-piperazinyl group (**3a**) showed the highest cytotoxicity against both OSCC cells and normal oral cells (mean CC_{50}=130 and 225 μM, respectively), followed by compound with 4-phenyl-1-piperidinyl (**2a**) (282; 228 μM), 4-morpholinyl (**5a**) (354; 318 μM), 1-piperidinyl (**1a**) (398; 366 μM) and 4-methyl-1-piperazinyl group (**4a**) (400; 396 μM) (Table I).

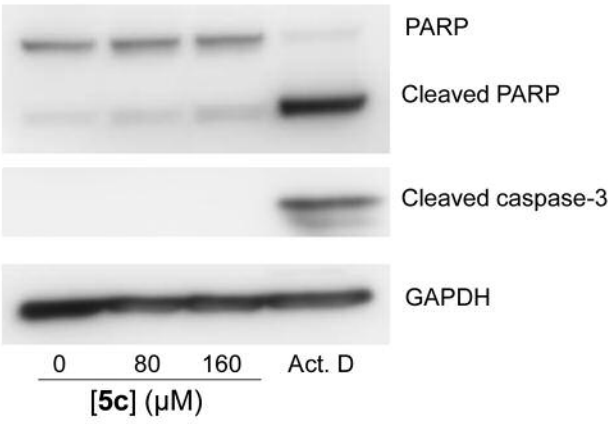

Figure 4. *Failure of caspase-3 activation by* ***5c*** *in HSC-2 cells. HSC-2 cells were incubated for 24 h with the indicated concentrations of* ***5c*** *or 1 μM actinomycin D (Act. D, positive control), and then investigated for apoptosis induction by western blot analysis.*

Introduction of methoxy group to a-series compounds at the C-6 position yielded b-series compounds. Four b-series compounds (**2b**, **3b**, **4b**, **5b**) except **1b** did not increase, but rather slightly reduced the cytotoxicity of the corresponding a-series compound (Table I).

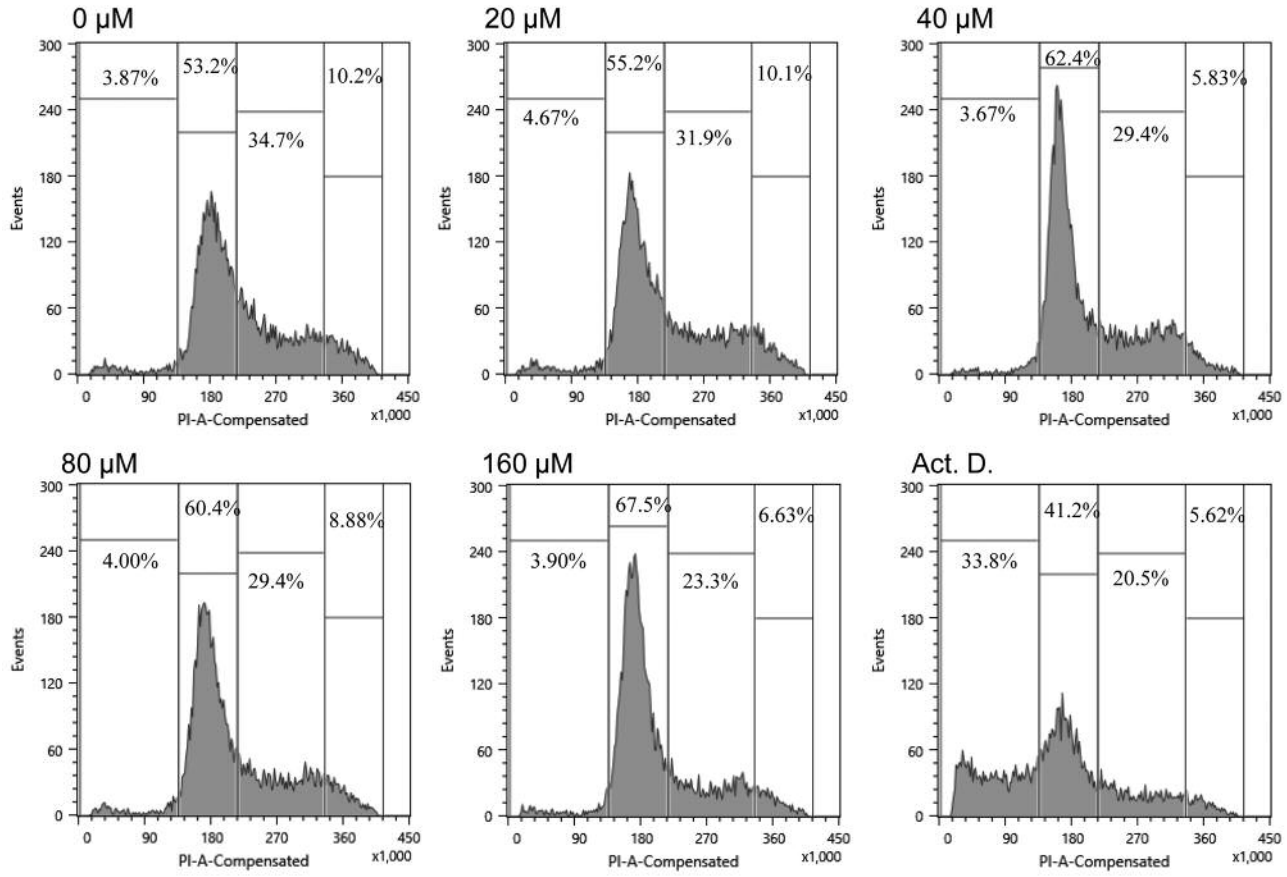

Figure 5. *Failure of production of subG$_1$ population by* ***5c****. Cell-cycle analysis of HSC-2 cells treated for 24 h with the indicated concentrations of* ***5c*** *or 1 μM actinomycin D (Act. D, positive control).*

Table II. *Number of descriptors that shows significant difference with T, N or T-N in ordinal condition (A), when* ***5c*** *was eliminated (B) or common in both A and B.*

	Number of descriptor that shows significant correlation with T, N or T-N (A)	Number of descriptors shows significant correlation with T, N or T-N when **5c** was eliminated (B)	Number of descriptors shows significant correlation with T, N or T-N (p<0.05) (common in A and B)
T	40	617	9
N	811	690	685
T-N	44	166	6

Introduction of methoxy group to a-series compounds at the C-7 position yielded c-series compounds. **5c** showed 63.3 (348/5.5)-fold higher cytotoxicity against OSCC cell lines as compared with (**5a**). **3c** showed 3.0 (275/93)-fold higher cytotoxicity as compared with **3a**. **1c**, **2c** and **4c** showed comparable cytotoxicity with (**1a**, **2a**, **4a**) (Table I).

Tumor-specificity. Tumor-specificity (TS) was calculated by dividing the mean CC_{50} value towards three normal cells by the mean CC_{50} value towards four OSCC cell lines (D/B, Table I). Among fifteen compounds, **5c** showed the highest tumor-specificity (TS=63.4), slightly higher than that of doxorubicin (TS=48.3). Dose-response curve of **5c** showed that it was

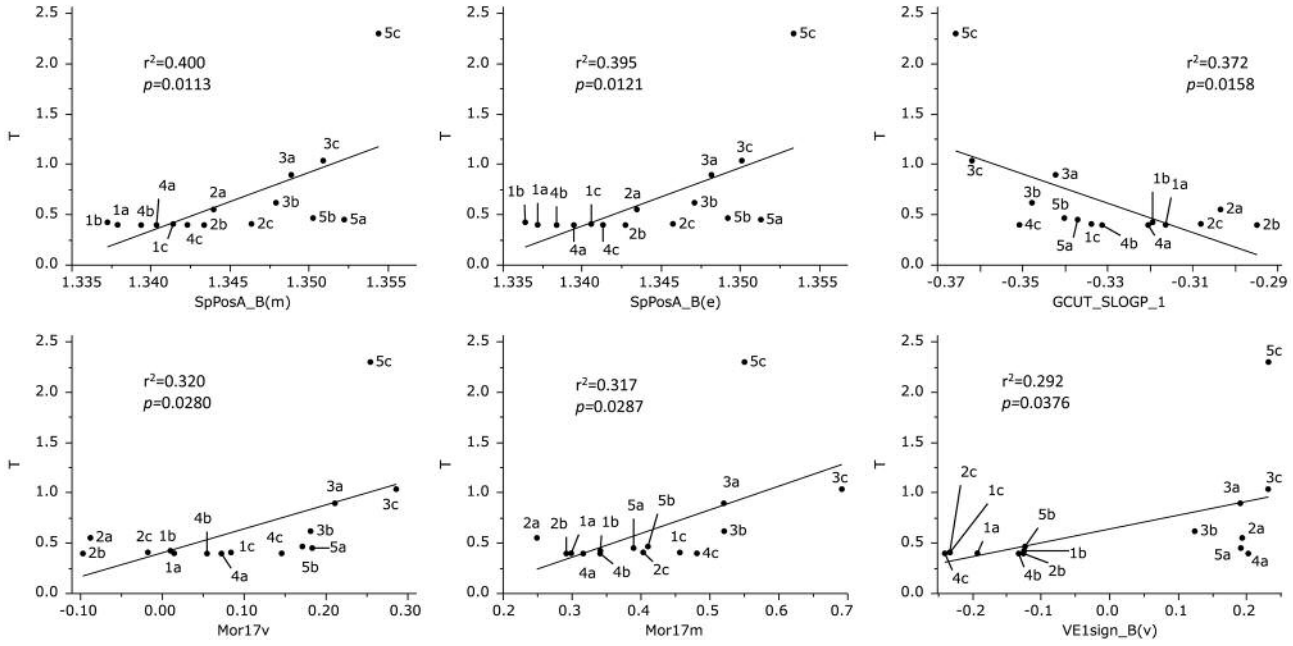

Figure 6. *Determination of coefficient between chemical descriptors and cytotoxicity of fifteen 2-(N-cyclicamino)chromones against tumor cells (defined as T). The mean (pCC_{50} i.e., the $-log\ CC_{50}$) values for tumor cell lines were defined as T.*

cytotoxic to OSCC cells, rather than cytostatic (Figure 2). **3c** showed some tumor-specificity (TS=3.0), whereas TS values of other 13 compounds were less than 2 (Table I).

Considering that HGF is the normal cell corresponding to cancer cell Ca9-22 (both derived from gingival tissues), TS values were also generated by dividing the average CC_{50} value towards HGF cells by the CC_{50} value towards Ca9-22 cells (C/A, Table I). **5c** (TS=26.7) showed again the highest tumor-specificity, only slightly lower than that of doxorubicin (TS=33.2). **3c** showed some tumor-specificity (TS=2.3) whereas TS values of other compounds were less than 2 (Table I).

PSE value. In order to identify the most promising compounds in terms of both good potencies and selectively cytotoxic, the potency-selectivity expression (PSE) values were calculated. **5c** showed more than 364-fold (1156.34/3.18) (calculated with all malignant and non-malignant cells; $(D/B_2)\times100$) or 108-fold higher PSE value (291.68/2.69) (calculated with cells from the same tissue; $(C/A^2)\times100$) than **3c** and other 13 compounds, although doxorubicin having lower CC_{50} values against OSCC cell lines showed much higher PSE values (Table I).

*Type of cell death induced by **5c***. When HSC-2 cells were incubated for 24 h with increasing concentrations (20, 40, 80 or 160 μM) of **5c**, cells became gradually enlarged (upper column in Figure 3). Cell enlargement and damage were more pronounced when incubation time was prolonged to 48 h (lower column in Figure 3). In contrast, actinomycin D (Act.D) treatment induced cell shrinkage, characteristic to apoptosis (Figure 3).

Western blot analysis demonstrated that **5c** did not produce caspase-3 activation, as evidenced by lack of cleavage of poly (ADP-ribose) polymerase (PARP) and capspase-3, in contrast to actinomycin D treatment (Figure 4).

Cell cycle analysis demonstrated that actinomycin D, but not **5c**, produced sub-G_1 cell population that is characteristic to apoptotic cells. **5c** increased the relative number of G_1 phase cells, while it reduced the number of S and M phase cells (Figure 5). These data reduced the possibility of apoptosis induction by **5c**.

Computational analysis. We next performed the QSAR analysis of fifteen 2-(*N*-cyclicamino)chromones in regards to their cytotoxicity against tumor cells and normal cells. Since **5c** shows remarkable tumor selectivity, we selected descriptors by two approaches, using all fifteen compounds or fourteen compounds excluding **5c**. We chose descriptors that show significant correlation with each of T, N, and T-N in both analyses (Table II). Among a total of 3089 descriptors, 13 descriptors correlated well with cytotoxicity and tumor specificity (Table III).

Cytotoxicity of fifteen 2-(*N*-cyclicamino)chromones against human OSCC cell lines was correlated positively with

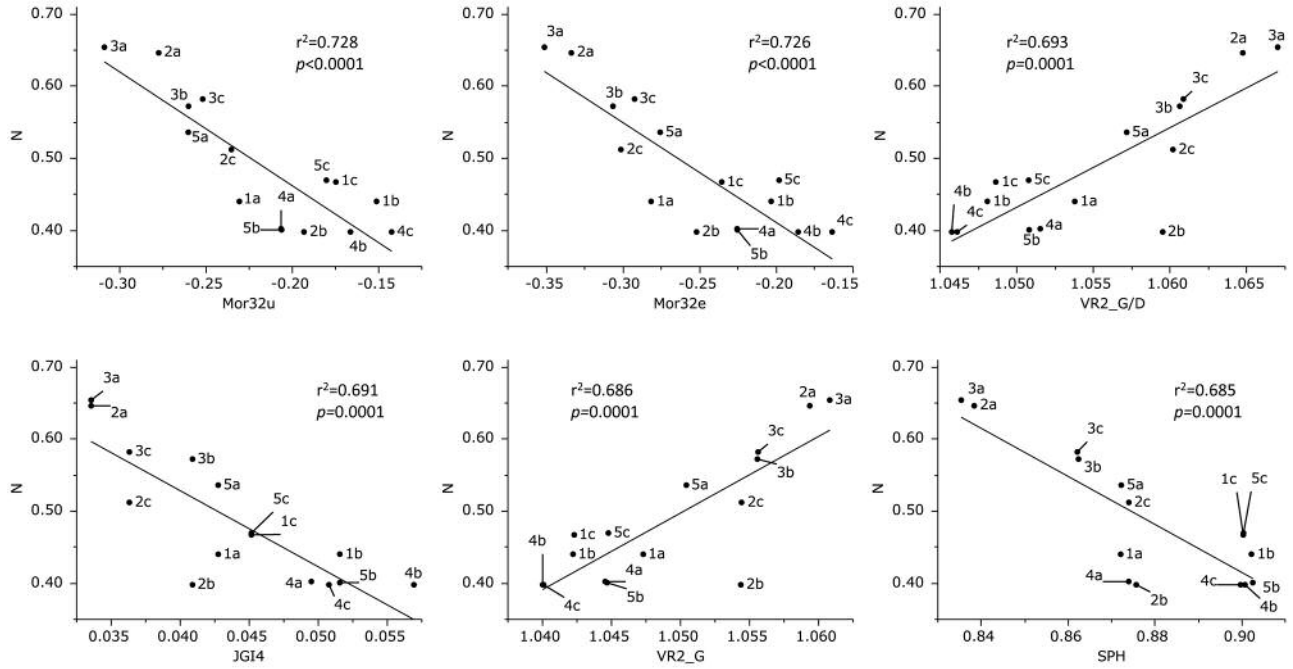

Figure 7. *Determination of coefficient between chemical descriptors and cytotoxicity of fifteen 2-(N-cyclicamino)chromones against normal cells (defined as N). The mean (pCC_{50} i.e., the $-log\ CC_{50}$) values for normal cells were defined as N.*

Table III. *Properties of descriptors that significantly affects the cytotoxicity against tumor cells (T), normal cells (N) and tumor-specificity (T-N).*

	Descriptor	Source	Meaning	Explanation
T	SpPosA_B(m)	Dragon	Topological shape and size	Normalized spectral positive sum from Burden matrix weighted by mass
	SpPosA_B(e)	Dragon	Topological shape and electric state	Normalized spectral positive sum from Burden matrix weighted by Sanderson electronegativity
	GCUT_SLOGP_1	MOE	Topological shape	The GCUT descriptors using atomic contribution to logP (using the Wildman and Crippen SlogP method) instead of partial charge. The GCUT descriptors are calculated from the eigenvalues of a modified graph distance adjacency matrix.
	Mor17v	Dragon	3D shape and size	Signal 17/weighted by van der Waals volume
	Mor17m	Dragon	3D shape and size	Signal 17/weighted by mass
	VE1sign_B(v)	Dragon	Topological shape and size	Coefficient sum of the last eigenvector from Burden matrix weighted by van der Waals volume
N	Mor32u	Dragon	3D shape	Signal 32/unweighted
	Mor32e	Dragon	3D shape and electric state	Signal 32/weighted by Sanderson electronegativity
	VR2_G/D	Dragon	3D shape	Normalized Randic-like eigenvector-based index from distance/distance matrix
	JGI4	Dragon	Topological shape and electric state	Mean topological charge index of order 4
	VR2_G	Dragon	3D shape	Normalized Randic-like eigenvector-based index from geometrical matrix
	SPH	Dragon	3D shape	Spherosity
T-N	Mor22m	Dragon	3D shape	Signal 22/weighted by mass
	GCUT_SLOGP_1	MOE	Topological shape	The GCUT descriptors using atomic contribution to logP (using the Wildman and Crippen SlogP method) instead of partial charge.The GCUT descriptors are calculated from the eigenvalues of a modified graph distance adjacency matrix.
	Mor17v	Dragon	3D shape and size	Signal 17/weighted by van der Waals volume
	Mor17m	Dragon	3D shape and size	Signal 17/weighted by mass

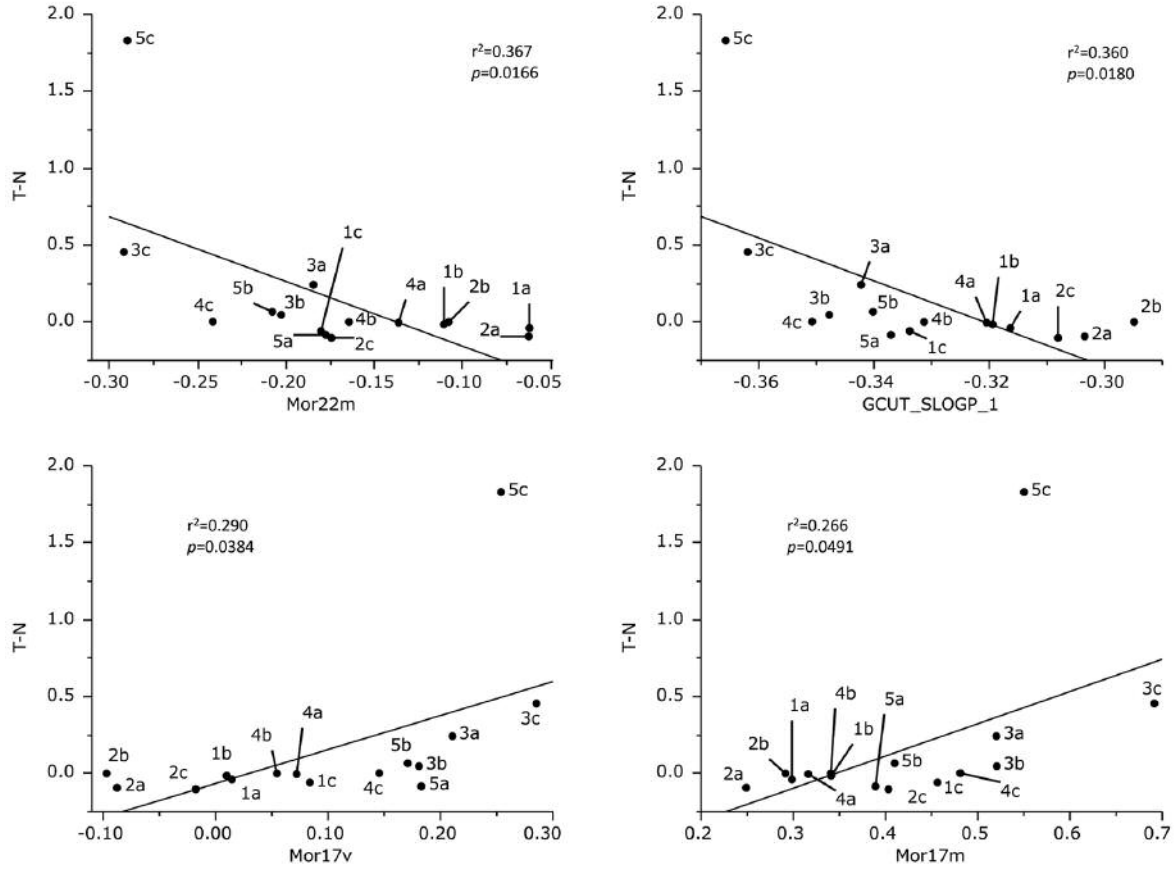

Figure 8. *Determination of coefficient between chemical descriptors and tumor specificity of fifteen 2-(N-cyclicamino)chromones (defined as T−N).*

SpPosA_B(m) (topological shape and size) (r^2=0.400, p=0.0113), SpPosA_B(e) (topological shape and electric state) (r^2=0.305, p=0.0121), Mor17v (3D shape and size) (r^2=0.320, p=0.0280), Mor17m (3D shape and size) (r^2=0.317, p=0.0287), VE1sign_B(v) (topological shape and size) (r^2=0.292, p=0.0376), while negatively with GCUT_SLOGP_1 (topological shape) (r^2=0.372, p=0.0158) (Figure 6).

Cytotoxicity of fifteen 2-(*N*-cyclicamino)chromones against human normal oral mesenchymal cells was correlated negatively with Mor32u (3D shape) (r^2=0.728, p<0.0001), Mor32e (3D shape and electoric state) (r^2=0.726, p<0.0001), JGI4 (topological shape and electric state) (r^2=0.691, p=0.0001), and SPH (shape) (r^2=0.685, p=0.0001) while positively with VR2_G/D (3D shape) (r^2=0.693, p=0.0001) and VR2_G (3D shape) (r^2=0.686, p=0.0001) (Figure 7).

Tumor specificity of fifteen 2-(*N*-cyclicamino)chromones was correlated negatively with Mor22m (3D shape) (r^2=0.367, p=0.0166) and GCUT_SLOGP_1 (topological shape) (r^2=0.360, p=0.0180), while positively with Mor17v (3D shape and size) (r^2=0.290, p=0.0384) and Mor17m (3D shape and size) (r^2=0.266, p=0.0491) (Figure 8).

Discussion

The present study demonstrated that among fifteen 2-(*N*-cyclicamino)chromones, 7-methoxy-2-(4-morpholinyl)-4*H*-1-benzopyran-4-one (**5c**) showed the highest tumor-specificity, comparable with that of doxorubicin (Table I). As far as we know, there is no report that has investigated the biological activity of this compound. Incubation of HSC-2 cells for 48 h with **5c** at 100 μM reduced the cell viability to 5% of control, suggesting its action seems to be cytotoxic rather than cytostatic. We concluded that **5c** did not induce apoptotic cell death, based on the next evidences: (i) it induced cell enlargement while actinomycin D induced cell shrinkage (Figure 3), (ii) it did not activate caspase-3 while actinomycin D induced activated caspase-3 (based on the induction of cleaved product of PARP and caspase-3) (Figure 4), (iii) it did not produce sub G_1 population while actinomycin D produced sub G_1 population (Figure 5). There are many types of cell death such as intrinsic and extrinsic apoptosis, oncosis, necroptosis, parthanatos, ferroptosis, sarmoptosis, autophagic cell death, autosis, autolysis, paraptosis, pyroptosis, phagoptosis,

and mitochondrial permeability transition (20). Further study is needed regarding which type of cell death **5c** induces in human OSCC cell lines.

QSAR analysis demonstrated that cytotoxicity of fifteen 2-(*N*-cyclicamino)chromones against tumor cell lines was correlated positively with SpPosA_B(m) (mass), SpPosA_B(e) (Sanderson electronegativity), Mor17v (van der Waals volume), Mor17m (mass), VE1sign_B(v) (van der Waals volume), while negatively with GCUT_SLOGP_1 (log P) (Figure 6). Their tumor specificity was reflected by Mor17v (van der Waals volume) and Mor17m (mass), while negatively with Mor22m (mass) and GCUT_SLOGP_1 (log P) (Figure 8). Taken together these data suggest that both their cytotoxicity against tumor cells and tumor-specificity are positively related with chemical descriptors that reflect molecular shape, especially 3D-structure (Figure 7). Chemical modification using **5c** as a lead compound may be a potential choice for designing a new type of anticancer drugs.

Conflicts of Interest

The Authors wish to confirm that there are no known conflicts of interest associated with this publication and there has been no significant financial support for this work that could have influenced its outcome.

Acknowledgements

This work was partially supported by KAKENHI from the Japan Society for the Promotion of Science (JSPS) (15K08111, 16K11519).

References

1 Gaspar A, Matos MJ, Garrido J, Uriarte E and Borges F: Chromone: a valid scaffold in medicinal chemistry. Chem Rev *114(9)*: 4960-4992, 2014.

2 Mazzei M, Sottofattori E, Dondero R, Ibrahim M, Melloni E and Michetti M: *N,N*-Dialkylaminosubstituted chromones and isoxazoles as potential anti-inflammatory agents.Il Farmaco *54*: 452-460, 1999.

3 Hatnapure GD, Keche AP, Rodge AH, Birajdar SS, Tale RH and Kamble VM: Synthesis and biological evaluation of novel piperazine derivatives of flavone as potent anti-inflammatory and antimicrobial agent. Bioorg Med Chem Lett *22(20)*: 6385-6390, 2012.

4 Abbott BM and Thompson PE: PDE_2 inhibition by the PI3 kinase inhibitor LY294002 and analogues. Bioorg Med Chem Lett *14*: 2847-2851, 2004.

5 Roma G, Di Braccio M, Grossi G, Piras D, Leoncini G, Bruzzese D, Signorello MG, Fossa P and Mosti L: Synthesis and *in vitro* antiplatelet activity of new 4-(1-piperazinyl)coumarin derivatives. Human platelet phosphodiesterase 3 inhibitory properties of the two most effective compounds described and molecular modeling study on their interactions with phosphodiesterase 3A catalytic site. J Med Chem *50(12)*: 2886-2895, 2007.

6 Raymond M, FinlayaRoger V and Griffinb J: Modulation of DNA repair by pharmacological inhibitors of the PIKK protein kinase family. Bioorg Med Chem Lett *22(17)*: 5352-5359, 2012.

7 Griffin RJ, Fontana G, Golding BT, Guiard S, Hardcastle IR, Leahy JJ, Martin N, Richardson C, Rigoreau L, Stockley M and Smith GC: Selective benzopyranone and pyrimido[2,1-a]isoquinolin-4-one inhibitors of DNA-dependent protein kinase: synthesis, structure-activity studies, and radiosensitization of a human tumor cell line *in vitro*. J Med Chem *48(2)*: 569-585, 2005.

8 Gao M, Wang M, Miller KD and Zheng QH: Simple synthesis of carbon-11-labeled chromen-4-one derivatives as new potential PET agents for imaging of DNA-dependent protein kinase (DNA-PK) in cancer. Appl Radiat Isot *70(8)*: 1558-1563, 2012.

9 Shimada C, Uesawa Y, Ishii-Nozawa R, Ishihara M, Kagaya H, Kanamto T, Terakubo S, Nakashima H, Takao K, Sugita Y and Sakagami H: Quantitative structure–cytotoxicity relationship of 3-styrylchromones. Anticancer Res *34*: 5405-5412, 2014.

10 Uesawa Y, Sakagami H, Ishihara M, Kagaya H, Kanamoto T, Terakubo S, Nakashima H, Yahagi H, Takao K and Sugita Y: Quantitative structure–cytotoxicity relationship of 3-styryl-2*H*-chromenes. Anticancer Res *35*: 5299-5308, 2015.

11 Sakagami H, Okudaira N, Uesawa Y, Takao K, Kagaya H and Sugita Y: Quantitative structure-cytotoxicity relationship of 2-azolylchromones. Anticancer Res *38(2)*: 763-770, 2018.

12 Sakagami H, Okudaira N, Masuda Y, Amano O, Yokose S, Kanda Y, Suguro M, Natori T, Oizumi H and Oizumi T: Induction of Apoptosis in human oral keratinocyte by doxorubicin. Anticancer Res *37(3)*: 1023-1029, 2017.

13 Takao K, Saito T, Chikuda D and Sugita Y: 2-Azolylchromone derivatives as potent and selective inhibitors of monoamine oxidases A and B. Chem Pharm Bull *64*: 1499-1504, 2016.

14 Samanta R, Narayan R, Bauer JO, Strohmann C, Sievers S and Antonchick AP: Oxidative regioselective amination of chromones exposes potent inhibitors of the hedgehog signaling pathway. Chem Commun *51*: 925-928, 2015.

15 Kantoh K, Ono M, Nakamura Y, Nakamura Y, Hashimoto K, Sakagami H and Wakabayashi H: Hormetic and anti-radiation effects of tropolone-related compounds. In Vivo *24*: 843-852, 2010.

16 Horikoshi M, Kimura Y, Nagura H, Ono T and Ito H: A new human cell line derived from human carcinoma of the gingiva. I. Its establishment and morphological studies. Jpn J Oral Maxillofac Surg *20*: 100-106, 1974.

17 Tomikoshi Y, Nomura M, Okudaira N, Sakagami H and Wakabayashi H: Enhancement of cytotoxicity of three apoptosis-inducing agents against human oral squamous cell carcinoma cell line by benzoxazinotropone. In Vivo *30(5)*: 645-650, 2016.

18 Calculate Descriptors, MOE2018.01 MOE user guide, Chemical Computing Group.

19 https://chm.kode-solutions.net/products_dragon_descriptors.php

20 Fricker M, Tolkovsky AM, Borutaite V, Coleman M and Brown GC: Neuronal Cell Death. Physiol Rev *98(2)*: 813-880, 2018.

Received May 19, 2018
Revised June 4, 2018
Accepted June 6, 2018